Eur. J. Mineral.
2009, **21**, 419–432
Published online March 2009

Zoning of laurite (RuS_2)–erlichmanite (OsS_2): implications for the origin of PGM in ophiolite chromitites

JOSÉ M. GONZÁLEZ-JIMÉNEZ[1,*], FERNANDO GERVILLA[1], JOAQUÍN A. PROENZA[2], THOMAS KERESTEDJIAN[3], THIERRY AUGÉ[4] and LAURENT BAILLY[4]

[1] Departamento de Mineralogía y Petrología and Instituto Andaluz de Ciencias de la Tierra (Universidad de Granada-CSIC), Facultad de Ciencias, Avda. Fuentenueva s/n, 18002 Granada, Spain
*Corresponding author, e-mail: jmgonzj@ugr.es
[2] Departament de Cristallografia, Mineralogia i Dipòsits Minerals, Facultat de Geologia, Universitat de Barcelona, Martí i Franquès s/n, 08028 Barcelona, Spain
[3] Geological Institute, Bulgarian Academy of Sciences, 24 Georgi Bonchev Str., 1113 Sofia, Bulgaria
[4] BRGM (Bureau de recherches géologiques et minières), Mineral Resources Division, 3 avenue Claude-Guillemin, BP 36009, 45060 Orléans cedex 2, France

Abstract: We have investigated several chromite deposits in the Mayarí-Baracoa Ophiolite Belt (eastern Cuba) and in the Dobromirtsi metamorphosed ultramafic (ophiolitic) massif (SE Bulgaria) with regard to zoning in platinum-group minerals (PGM) of the laurite (RuS_2)–erlichmanite (OsS_2) solid solution series. We found several zoned laurite–erlichmanite grains all included in unaltered chromite crystals. On the basis of internal ordering and compositional variations, three different patterns of zoning have been distinguished: (i) grains with Os-poor (laurite) core and Os-rich rim (normal zoning), (ii) grains with Os-rich core and Os-poor rim (reverse zoning) and (iii) grains made up of a complex intergrowth of Os-rich, Os-poor laurite and erlichmanite (oscillatory zoning). The origin of zoning is interpreted mainly as a result of changes in $f(S_2)$, $f(O_2)$ and to a lesser extent in melt temperature, before PGM trapping in chromite. A possible case of heterogeneous physicochemical environment in which such changes can take place is when chromite forms during magma mingling of silicate melts in the upper mantle. The preservation of laurite–erlichmanite zoning is attributed to the low diffusion coefficient of Ru and Os in pyrite-type structures.

Key-words: platinum-group minerals (PGM), laurite–erlichmanite zoning, ophiolite complex, chromitite, magma mixing, Mayarí-Baracoa Ophiolite Belt, Dobromirtsi Ultramafic Massif.

1. Introduction

The platinum-group minerals (PGM) of the laurite (RuS_2)–erlichmanite (OsS_2) solid solution series are the most common PGMs in podiform chromite ores that are hosted by mantle peridotites in ophiolite complexes. They represent 75% of the total PGM described in this type of ores (based on our unpublished statistical analysis of literature). They occur mainly as small (usually below 20 μm) mineral inclusions in chromite, forming anhedral to euhedral crystals, in single or composite grains, associated with other PGMs, base-metal sulphides and/or silicates (Stockman & Hlava, 1984; Legendre & Augé, 1986; Augé & Johan, 1988; Corrivaux & Laflamme, 1990; Torres-Ruiz *et al.,* 1996; Melcher *et al.,* 1997; Garuti *et al.,* 1999a, b; Ahmed & Arai, 2003a, b; Gervilla *et al.,* 2005; among others). Most authors agree that laurite–erlichmanite grains form at high temperature from sulphur-undersaturated mafic melts, before or coeval with the crystallization of chromite. They may crystallize directly from the melt, acting as nuclei for chromite crystallization (Stockman & Hlava, 1984; Augé, 1985) or as the result of the reaction of previously formed Os-Ir-Ru alloys with sulphur, when fS_2 increases in the melt (Bockrath *et al.,* 2004). The Os-Ir-Ru alloys may crystallize attached to chromite grain boundaries (Bockrath *et al.*, 2004; Mungall, 2005; Ballhaus *et al.*, 2006; Finnigan *et al.*, 2008), also being found commonly within chromite crystals. Growing chromite tends to trap these PGMs, preventing any further chemical exchange with the melt (Stockman & Hlava, 1984; Gauthier *et al.*, 1990; Bockrath *et al.*, 2004). Because the composition of laurite–erlichmanite is strongly influenced by sulphur fugacity and temperature (Brenan & Andrews, 2001; Andrews & Brenan, 2002; Bockrath *et al.*, 2004), each individual, sealed inclusion records valuable information on the thermodynamic conditions prevailing during its crystallization (Augé & Johan, 1988; Nakagawa & Franco, 1997; Garuti *et al.*, 1999a).

The identification of complex oscillatory zoning patterns in laurite–erlichmanite crystals from two chromite

0935-1221/09/0021-1921 $ 6.30
DOI: 10.1127/0935-1221/2009/0021-1921

deposits in the Mayarí-Baracoa Ophiolitic Belt (eastern Cuba), as well as other simple patterns made up of two individuals: core + rim, in zoned grains from metamorphosed chromitites of the Dobromirtsi Ultramafic (ophiolite) Massif in the Rhodope Mountains (SE Bulgaria) is a good opportunity to investigate the variations of the physico-chemical conditions that control the formation of these PGMs during the crystallization of chromite. For this study, we have selected only laurite–erlichmanite grains occurring in unaltered, unfractured chromite crystals to make sure that the primary features of the zoning patterns were not modified by late alteration processes. These features will be compared with those of zoned laurite–erlichmanite grains described in the literature Corrivaux & Laflamme, 1990; Melcher *et al.*, 1997; Garuti *et al.*, 1999a; Gutierrez-Narbona *et al.*, 2003; Zaccarini *et al.*, 2004; Gervilla *et al.*, 2005; Grieco *et al.*, 2006).

2. Geological setting of the sampled areas

The samples were selected from two chromite ore bodies (Monte Bueno and Caridad Mines) in Sagua de Tánamo District, eastern Cuba (Proenza *et al.*, 1999; Gervilla *et al.*, 2005) and ten chromitite occurrences from the Dobromirtsi Ultramafic Massif in SE Bulgaria (Tarkian *et al.*, 1991; Kerestedjian *et al.*, 2006; González-Jiménez *et al.*, 2007).

The Sagua de Tánamo District is a small mining district, located in the central part of the Late Cretaceous Mayarí-Baracoa Ophiolitic Belt (Marchesi *et al.*, 2006; Proenza *et al.*, 2006), in an area with a complex structure characterized by the imbrication of different tectonic sheets of ophiolite-related, mainly serpentinized ultramafic rocks (Fig. 1a). Ophiolite-related, ultramafic rocks are mainly composed of serpentinized mantle tectonites made up of harzburgite and minor dunite. Harzburgite contains anhedral to amoeboid crystals of chrome spinel (< 2 vol%), while dunite shows more abundant euhedral accessory chromite crystals (> 2 vol%). The emplacement of the ophiolite took place in the Maastrichtian to early Danian (Iturralde-Vinent *et al.*, 2006). This district contains 35 small deposits of both Al-rich (25 deposits) and Cr-rich (10 deposits) chromite ore (Murashko & Lavandero, 1989; Proenza *et al.*, 1999, 2003). Chromitite bodies are relatively small (but any of them contains more than 100,000 tons of chromite ore) and have irregular, tabular to

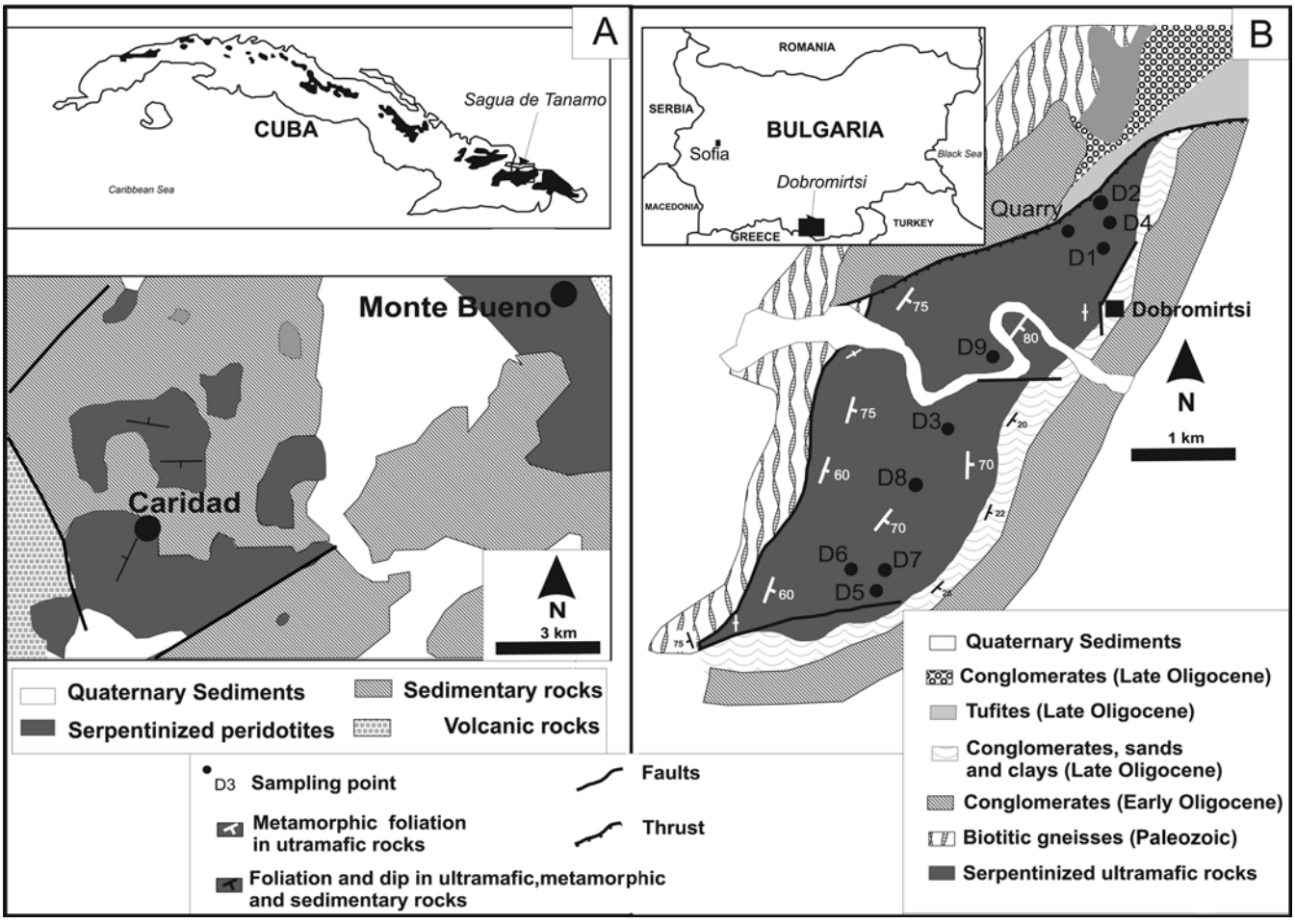

Fig. 1. Geological maps of a portion of the Sagua de Tanamo district (a) and Dobromirtsi Ultramafic Massif (b) with the location of the studied chromitites.

lenticular shapes. They are concordant or subconcordant with the foliation of the host serpentinized peridotites (mantle harzburgites with dunite lenses hosting chromitites; Proenza *et al.*, 1999, 2003; Gervilla *et al*., 2005) and are locally cut and rotated by normal faults. Chromitites show massive textures, frequently grading to disseminate towards the borders of the bodies; much less frequently they have banded and disseminated textures.

The Dobromirtsi Ultramafic Massif is a small ultramafic body (~11 km^2) located in the Borovitza lithotectonic unit – the uppermost unit of the Variegated Complex – in the Central Rhodopes (Ovtcharova *et al.*, 2001). It is mainly composed of serpentinized harzburgites and dunites, metamorphosed under amphibolite-facies conditions, which are considered part of the mantle section of a dismembered Paleozoic Ophiolite Complex (Ovtcharova *et al*., 2001) (Fig. 1b). Almost 200 chromitite podiform bodies of variable, but small size (only a few of them contain some tens of thousands tons of ore) can be found in this massif (Zhelyaskova-Panayotova, 2000). They are all concordant to the metamorphic, mylonitic foliation of the host peridotites and concentrate in a single, dunite-rich horizon. Chromitites are predominantly massive, grading to disseminated towards the borders of the bodies.

3. Analytical methods

Polished thin-sections were studied in reflected light, by environmental scanning electron microscopy (ESEM) at the Centro Andaluz de Medio Ambiente (University of Granada-Junta de Andalucía) and field emission scanning electron microscopy (FESEM) at the Centro de Instrumentación Científica (University of Granada), to identify zoned laurite–erlichmanite grains. The larger grains were later analyzed by electron microprobe at the Serveis Cientificotécnics of the University of Barcelona and at the Analysis and Mineral Characterisation Laboratory of BRGM (Orléans, France). In both laboratories, analyses were obtained using CAMECA SX50 instruments, under the same operating conditions: accelerating voltage 25 kV, sample current 20 nA and beam diameter 2 μm. The X-ray lines measured were $K\alpha$ for S, Fe, Ni and Cr; $L\alpha$ for Ru, Rh, Pd, Os, Ir and Pt; and $L\beta$ for As. Pure metals were used as standards for Os, Ir, Ru, Rh, Pt, Pd and Ni, Cr_2O_3 for Cr, FeS_2 for Fe and S, Cu_2S for Cu, and GaAs for As. The following interferences Ir$L\alpha$→Cu$K\alpha$, Ru$L\beta$→Rh$L\alpha$, Cu$K\beta$→Os$L\alpha$, were corrected online. At BRGM, the Ru$L\beta$→Rh$L\alpha$ interference was corrected considering that 100% Ru corresponds to 2.3% Rh.

A total of 10 zoned laurite–erlichmanite grains were identified (all of them in unaltered chromite) in the studied chromitites: six in the Monte Bueno Mine, one in the Caridad Mine, and three in the Ultramafic Dobromirtsi Massif. Due to the small size of the grains and very fine scale of zoning, only three of the ten grains could be analyzed with microprobe. Despite the effort to analyze different zones of the grains with a maximum range of Os and Ru-variation, the performed analyses show a slight contamination as a consequence of mixing among the different zones. As a result, no correction can be done in this respect. Thus, the provided representative analyses represent average composition of a portion of representative Os- and/or Ru rich zones that form the grains. Also, raw PGM analyses showed moderate to significant concentrations of Fe and Cr due to excitation of the matrix, because of the small size of the particle. These data were corrected, by subtraction of Cr and the corresponding proportion of Fe due to the chromite (determined from the known Cr/Fe ratio, measured in the host chromite) from the raw analytical data, and the atomic concentration was calculated from the corrected analytical data (Augé, 1988). Since laurite could contain some amounts of Pt, Rh, Ni and Fe (Cabri, 2002), for the calculation of the structural formulae all these elements were also considered.

4. Patterns of zoning

Different zoned laurite–erlichmanite grains were found in the chromite ore bodies of the Monte Bueno and Caridad mines in the Sagua de Tánamo District (Table 1). The grains from Monte Bueno Mine exhibit oscillatory zoning, represented by alternating growth zones (parallel to growing crystal faces) of variable thickness and composition,

Table 1. Zoned laurite-erlichmanite grains in the studied chromitites.

Occurrence	Locality	Compositional zoning (core-rim)	Attached mineral	Pattern of zoning	Fig./Anal.
Monte Bueno	Sagua de Tánamo (Eastern Cuba)	Laurite/Os-laurite/laurite/irarsite/laurite		Oscillatory	2a, 5/1–4
		Os-laurite/laurite/irarsite/laurite/irarsite		Oscillatory	2b
Caridad	Sagua de Tánamo (Eastern Cuba)	Os-laurite/laurite	Cuproiridsite	Oscillatory	4, 5/20–30
Dobromirtsi	Rhodopes (Southeastern Bulgaria)	Os-laurite/laurite	PGE-rich mss	Reverse	2c, 5/5–8
		Os-laurite/laurite		Reverse	
		Os-laurite/laurite	Osmium	Oscillatory	2d, 5/10–19

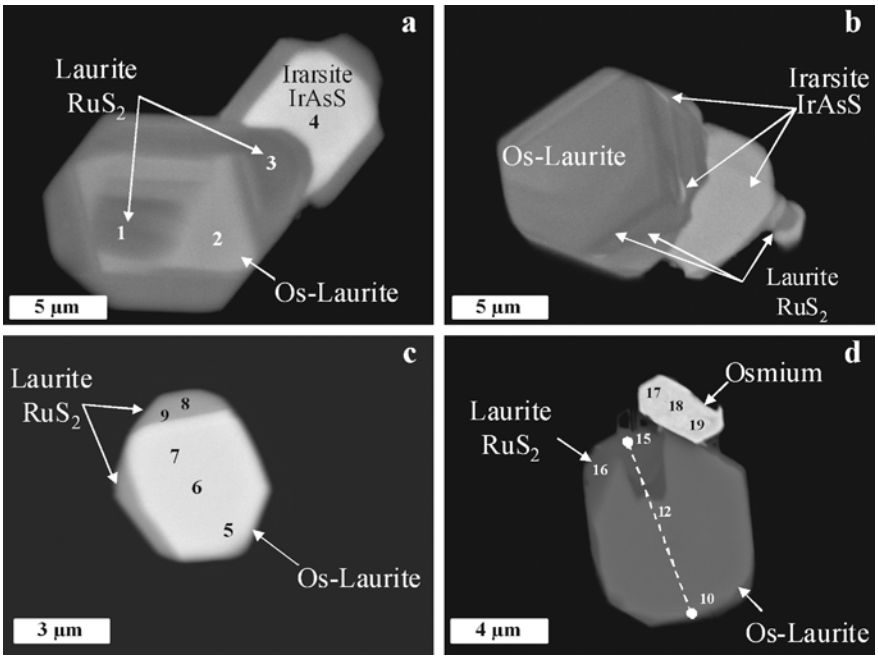

Fig. 2. Back-scattered images of zoned laurites included in chromite crystals. (a) and (b): Complex oscillatory zoned grains from the Monte Bueno Mine. Note that alternating bands of Os-poor and Os-rich laurite in both grains are of variable thickness and commonly parallel to crystal faces being interlayered or interrupted at the external boundary of the grains by irarsite. (c) and (d), Simple zoned grains from the Dobromirtsi Ultramafic Massif showing reverse zoning patterns. In figure (d), an irregular Os-rich laurite core is surrounded by thin, growth-related bands of laurite progressively poorer in Os content. Numbers indicate the analyses performed (Table 3).

that extend from Os-poor laurite to Os-rich laurite (Fig. 2a, b). A clear trend is observed in the crystal shape depending on composition, from octahedral in Os-rich zones to cub-octahedral for the pure laurite zones. Another specific feature of these laurite–erlichmanite grains is that at certain growth zones (corner and edges) subhedral irarsite crystals occur (Fig. 2a, b).

Another zoned grain from the Monte Bueno Mine is described by Gervilla *et al.* (2005) (Table 2) who shows that the core is made up of small, rounded (or corroded) grains (Fig. 3a), evidencing either the simultaneous formation of different nuclei of Os-rich laurite (or erlichmanite) or the effects of dissolution processes before the crystallization of the alternating, external zones. In addition this grain also has an irarsite crystal growing on the corner of a cub-octahedral individual.

Although a laurite–erlichmanite grain from the Caridad Mine shows a simple pattern of zoning (Fig. 4), there are some interesting features: i) it contains several drop-like to subhedral inclusions of (Ni,Cu,Fe) sulphides (mainly millerite, chalcocite and pentlandite), aligned along growth zones of the host laurite; ii) the laurite crystal is intergrown with an unknown PGE-rich monosultide solid solution (mss) (associated with a grain of cuproiridsite), causing a zone of compositional uniformity parallel to the assimilation boundary.

Three primary zoned laurite grains were found in two of the ten investigated chromitite bodies in the Dobromirtsi Ultramafic Massif. Two of them exhibit simple patterns of zoning (Fig. 2c) and the third one shows a corroded Os-laurite core rimmed by thin laurite zones (Fig. 2d). This photograph also shows a crystal of native Os attached to the outermost laurite rim.

5. Chemical variations

The chemical composition of zoned grains of laurite–erlichmanite from Sagua de Tánamo, Dobromirtsi and those reported in the literature show that zoning is mainly caused by changes in the Ru/(Ru+Os) ratio (from 0.99 to 0.27) with minor Ir variations (Fig. 5).

The only analyzed grain from Monte Bueno Mine (Fig. 2a) shows a core of Os-poor laurite $[(Ru_{0.87}Os_{0.11}Ir_{0.05}Rh_{0.01})_{\Sigma=1.03}S_{1.97}]$ surrounded by a zone of Os-rich laurite $[(Ru_{0.61}Os_{0.36}Ir_{0.05}Rh_{0.01})_{\Sigma=1.02}S_{1.98}]$ and an outermost rim of Os-poor laurite $[(Ru_{0.86}Os_{0.10}Ir_{0.04}Rh_{0.03})_{\Sigma=1.03}(S_{1.93}As_{0.04})_{\Sigma=1.97}]$ (Fig. 5; Table 3). In contrast, the laurite grain from Caridad (Fig. 4) exhibits a simpler pattern with a slightly Os enriched core $[(Ru_{0.66}Os_{0.24}Ir_{0.06}Rh_{0.01})_{\Sigma=0.98}S_{2.02}]$ and an Os poorer rim $[(Ru_{0.72}Os_{0.18}Ir_{0.08}Rh_{0.01}Ni_{0.01})_{\Sigma=0.99}S_{2.01}]$. Note that whereas Ru contents do not vary significantly along the profile of Fig. 4 (Table 3), Os depletion in the outer zone is accompanied by a slight increase in Ir content.

The two zoned grains from Dobromirtsi show very similar core to rim chemical variations (Fig. 5), having Os-rich laurite cores and Os-poor laurite rims. These compositions vary from $(Ru_{0.69}Os_{0.27}Ir_{0.03}Fe_{0.03}Rh_{0.01})_{\Sigma=1.02}S_{1.98}$ (core) to $(Ru_{0.91}Os_{0.07}Ir_{0.02})_{\Sigma=1.01}S_{1.99}$ (rim)

Table 2. Zoned laurite-erlichmanite from ophiolite and orogenic lherzolite massifs worldwide.

Occurrence	Locality	Compositional zoning (core-rim)	Attached mineral	Pattern of zoning	Fig.	References
Monte Bueno	Sagua de Tánamo (Eastern Cuba)	Erlichmanite/laurite/ Os-laurite	Irarsite	Oscillatory	3a	Gervilla *et al*. (2005)
Victoria	Mayarí (Eastern Cuba)	Erlichmanite/laurite/ Os-laurite		Oscillatory	3f, 5	Gervilla *et al*. (2005)
Nurali	Southern Urals (Russia)	Laurite-erlichmanite		Reverse	2b,5	Zaccarini *et al*. (2004)
		Erlichmanite-laurite		Oscillatory		Grieco *et al*. (2006)
		Laurite-erlichmanite		Normal		
		Erlichmanite/Ru-rich erlichmanite		Reverse		
		Laurite/Os-laurite		Normal		
		Laurite/Os-laurite/ erlichmanite/laurite		Oscillatory	3e, 5	
Ojén	Spain	Os-laurite/laurite		Reverse		Torres-Ruiz *et al*. (1996)
		Laurite/Os-laurite		Normal		
		Os-laurite/laurite		Normal	3c, 5	Gutierrez-Narbona *et al.* (2003)
Ray-Iz	Polars Urals (Russia)	Laurite/Os-laurite	Os-Ir alloy	Normal	5	Garuti *et al*. (1999a, b)
Thetford Mines	Canada	Os-laurite/laurite	Os/Ir alloy	Reverse	3d, 5	Corrivaux & Laflamme (1990)
Kempirsai	Kazakhstan	Os-laurite/laurite		Reverse		Melcher *et al*. (1997)

(Fig. 2c), and from $(Ru_{0.74}Os_{0.22}Ir_{0.05}\ Fe_{0.03})_{\Sigma=1.03}S_{1.97}$ (core) to $(Ru_{0.96}Os_{0.05}Ir_{0.02}Fe_{0.02}Rh_{0.01})_{\Sigma=1.06}S_{1.94}$ (rim) (Fig. 2d). The osmium attached to the outermost rim of the latter inclusion contains 78.71 wt% Os, 16.02 wt% Ir and 3.92 wt% Ru on average.

Primary zoned laurite-erlichmanite grains with significant core to rim variations grains are also described in other podiform chromitites (Table 2; Fig. 5). Most of these grains show simple patterns of zoning (*e.g.*, Fig. 3b, c, d; Fig. 5): Ray-Iz [from $(Ru_{1.00}Os_{0.02}Ir_{0.03})_{\Sigma=1.05}S_{1.95}$ to $(Ru_{0.72}Os_{0.14}Ir_{0.07}Rh_{0.0}Pt_{0.01})_{\Sigma=0.97}S_{2.03}$; Garuti *et al*., 1999a]; Ojén [from $(Ru_{0.71}\ Ir_{0.12}\ Rh_{0.10}Os_{0.09})_{\Sigma=1.02}\ (S_{1.79}As_{0.219})_{\Sigma=1.98}$ to $(Ru_{0.59}Os_{0.17}Ir_{0.13}\ Rh_{0.10})_{\Sigma=1.00}(S_{1.80}As_{0.20})_{\Sigma=2.00}$; Gutiérrez-Narbona *et al*., 2003]; Nurali [from $(Ru_{0.84}Os_{0.13}Ir_{0.02}Fe_{0.01}Ni_{0.01})_{\Sigma=1.00}S_{2.00}$ to $(Os_{0.90}Ru_{0.07}Ni_{0.04}Fe_{0.02})_{\Sigma=1.03}(S_{1.94}As_{0.03})_{\Sigma=1.97}$ and from $(Os_{0.69}Ru_{0.26}Ir_{0.02}Fe_{0.02}Ni_{0.01})_{\Sigma=0.99}S_{2.01}$ to $(Os_{0.54}Ru_{0.39}Ir_{0.03}Fe_{0.01}Ni_{0.01})_{\Sigma=0.99}S_{2.01}$; Zaccarini *et al*., 2004], and Thetford Mines [from $(Ru_{0.56}Os_{0.32}\ Ir_{0.08})_{\Sigma=0.96}S_{2.04}$ to $(Ru_{0.62}Os_{0.20}Ir_{0.08})_{\Sigma=0.89}S_{2.11}$; Corrivaux & Laflamme, 1990]. However, the most significant chemical variations in oscillatory zoned laurite–erlichmanite grains included in unaltered chromite are those reported by Grieco *et al*. (2006) in chromitites from the Nurali ophiolite (Fig. 3e). These authors describe an oscillatory zoned grain with an Os-poor laurite core $[(Ru_{0.86}Os_{0.09}Ir_{0.04}Rh_{0.01}Fe_{0.01}Ni_{0.01})_{\Sigma=1.02}S_{1.98}]$ surrounded by alternating zones of laurite with increasing amounts of Os, entering the compositional field of erlichmanite [up to $(Os_{0.63}Ru_{0.43}Ir_{0.04}Rh_{0.01})_{\Sigma=1.11}S_{1.89}$]. The outermost rim of this grain is again rich in Ru $[(Ru_{0.73}Os_{0.33}Ir_{0.03}Ni_{0.01})_{\Sigma=1.10}S_{1.90}]$. In addition to these primary patterns, Gervilla *et al*. (2005) report an oscillatory zoned grain in an open inclusion, located close to the border of a chromite crystal from the Victoria Mine (Mayarí District, eastern Cuba) (Fig. 3f). This grain has a partly rounded core surrounded by alternating growth zones. In spite of its textural position, this grain does not show any evidence of late alteration and its pattern of zoning could be considered primary.

6. Discussion

There is a general consensus among researchers on the primary, magmatic origin of PGMs occurring in sealed inclusions in unaltered chromite. Thus the three basically different patterns of zoning described in laurite–erlichmanite: i) grains with Os-poor (laurite) cores and Os-rich rims, ii) grains with Os-rich cores and Os-poor rims, and iii) grains with oscillatory patterns, must be formed during crystallization of chromite. Because a progressive increase in the Os content of laurite would be expected on cooling as a consequence of both decreasing temperature and increasing fS_2 (Stockman & Hlava, 1984; Augé & Johan, 1988; Melcher *et al*., 1997; Garuti *et al*., 1999a) we have termed the first type of pattern normal and the second one reverse (see Tables 1 and 2).

Two questions arise in our attempt to understand the different patterns of zoning: i) how do chemistry and/or thermodynamic conditions change to give rise to such different patterns of zoning? and ii) why did zoning not disappear by Os and Ru diffusion on cooling?

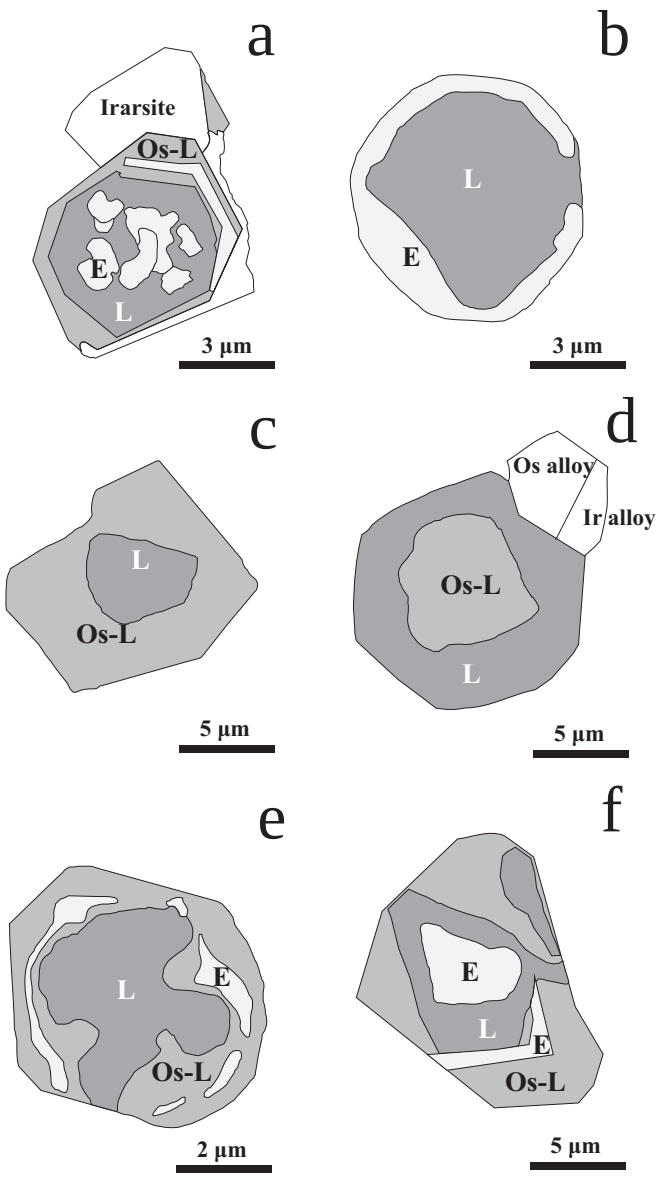

Fig. 3. Different examples of zoned laurites included in unaltered chromites from ophiolite and orogenic-lherzolite chromitites worldwide. (a) Complex oscillatory zoned grain from Monte Bueno Mine (Mayarí-Baracoa belt, eastern Cuba) (Gervilla *et al*., 2005) showing a core made up of small, rounded or corroded grains of erlichmanite (E) surrounded by external bands of Os-poor laurite (L) interlayered with thin bands of erlichmanite and/or Os-rich laurite (Os-L) finally interrupted by the crystallization of an irarsite crystal. (b) Simple zoned grain from Nurali, Russia (Zaccarini *et al*., 2004) showing a normal pattern of zoning composed of a core of laurite and a rim of erlichmanite. (c) Simple zoned grain from Ojén, Spain (Gutierrez-Narbona *et al*., 2003) showing a normal pattern of zoning, made up of Os-poor laurite core gradding to Os-rich laurite edge. (d) Simple (reverse zoning) zoned grain from Thetford Mines, Canada (Corrrivaux & Laflamme, 1990) composed of an Os-rich laurite core and an Os-poor laurite rim. (e) Complex oscillatory zoned grain from Nurali, Russia (Grieco *et al.*, 2006) showing a corroded core of Os-poor laurite enveloped by Os-rich laurite intergrown with a layer of erlichmanite. (f) Complex oscillatory zoned grain from Victoria mine (Mayarí-Baracoa belt, eastern Cuba) (Gervilla *et al*., 2005) showing an Ru-rich erlichmanite core surrounded by alternating, growth-related bands of Os-poor and Os-rich laurite.

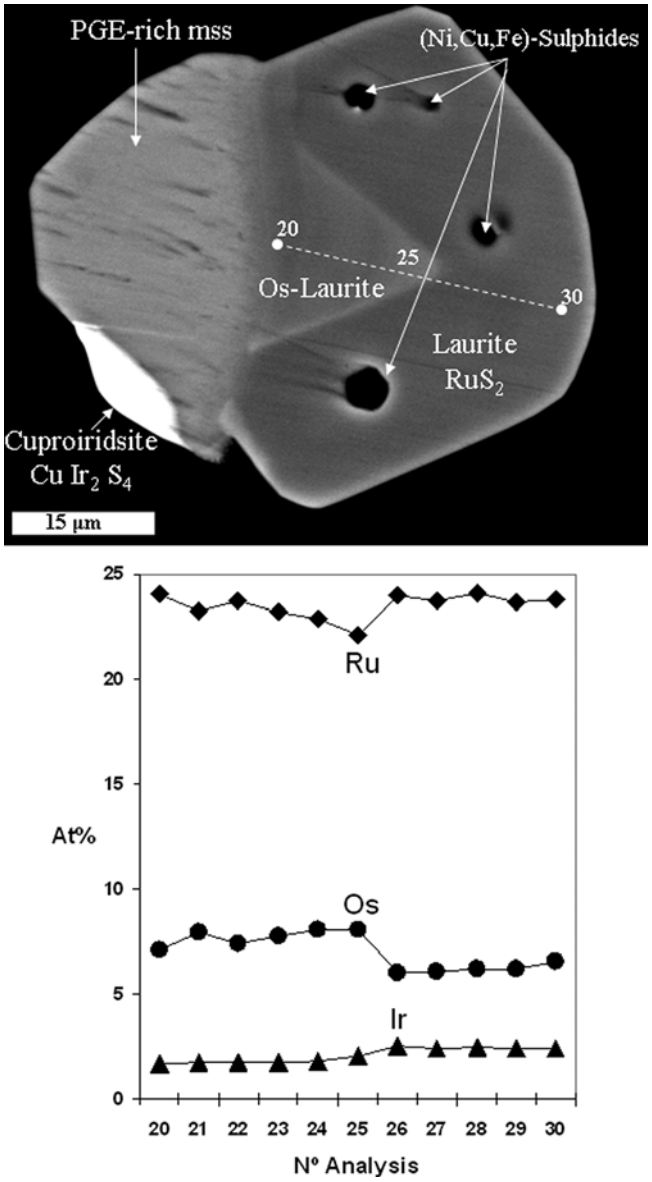

Fig. 4. Back-scattered image and compositional profiles of a composite grain from the Caridad Mine, made up of zoned laurite to which one crystal of a PGE-rich mss and one grain of cuproiridsite are associated. Note that the oscillatory zoned laurite grain has a Os-rich laurite core surrounded by an Os-poor rim hosting several drop-like to subhedral inclusions of Ni-Fe-Cu sulphides. The latter are oriented according to the growth band of the host laurite.

6.1. Origin of zoning

Experimental results indicate that Os, Ir and Ru fractionate into chromite and are later exsolved from the host chromite to form PGM inclusions (Capobianco & Drake, 1990; Capobianco *et al*., 1994; Righter *et al*., 2004); however, empirical observations (Tredoux *et al*., 1995) along with LA-ICP-MS analyses (Ballhaus & Sylvester, 2000) and recent experimental data (Matveev & Ballhaus, 2002; Sattari *et al*., 2002; Bockrath *et al*., 2004; Mungall, 2005; Finnigan *et al.,* 2008) show that the concentration of Os, Ir,

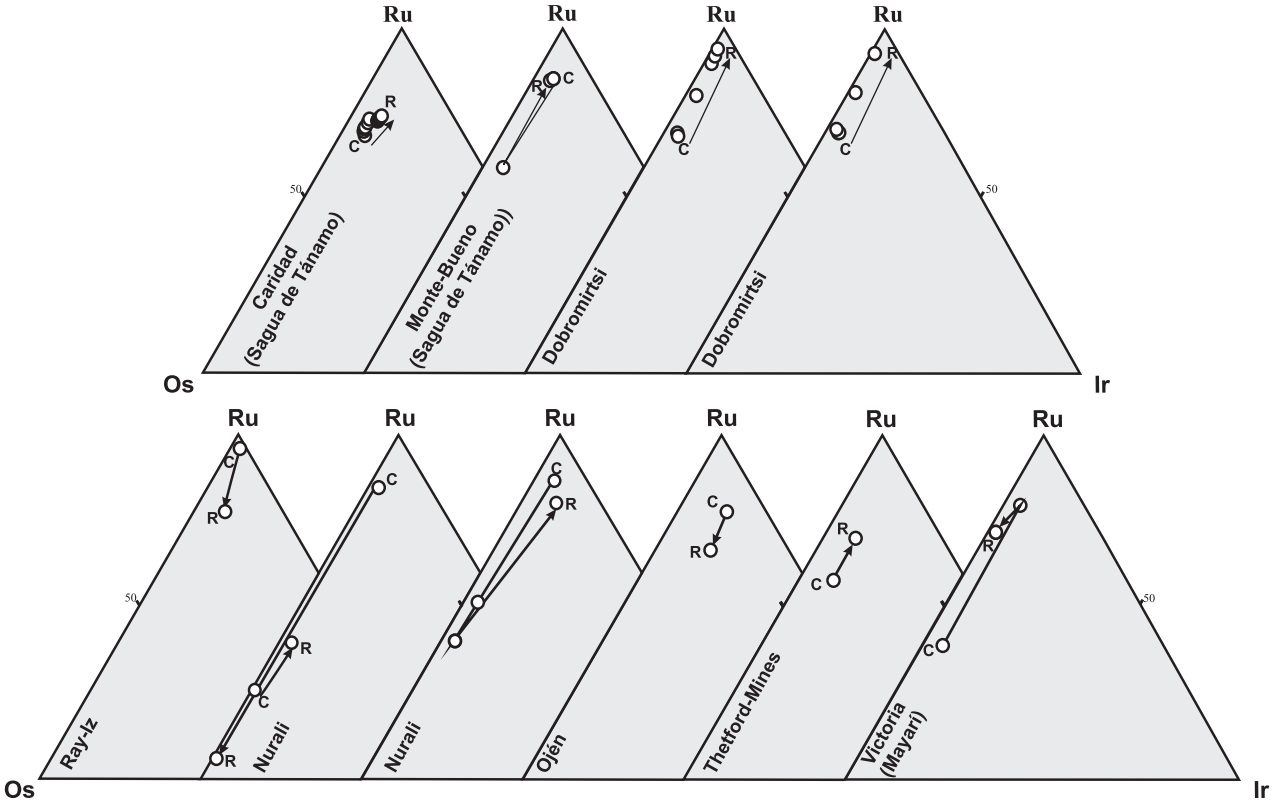

Fig. 5. Ru-Os-Ir plots of the zoned laurite–erlichmanite grains from the investigated chromitites and from the ophiolite and orogenic-lherzolite complexes worldwide. C: cores, R: rims. Arrows indicate compositional variation from cores to rims. References in the text.

and Ru in chromite is likely due to a physical trapping of submicroscopic clusters of these PGE in their metallic state, together with larger grains of PGM alloys and sulphides. Segregation of PGE clusters and PGMs from the melt is caused by changes in fO_2, fS_2 and temperature (Stockman & Hlava, 1984; Amossé *et al*., 1990, 2000; Mungall, 2002, 2005); thus, it would be expected that Os, Ir and Ru metallic clusters and alloys form first, under high temperature and low fS_2, followed by sulphides of the laurite–erlichmanite solid-solution series upon cooling and increasing fS_2 (Augé & Johan, 1988; Garuti *et al.*, 1999a). However, Brenan & Andrews (2001) and Bockrath *et al*. (2004) have shown that Os-Ir alloys can form in equilibrium with Os-free laurite at 1200–1300 °C and log fS_2 from −2 to −1.3. These results, in agreement with thermodynamic data (Stockman & Hlava, 1984; Wood, 1987; Barin, 1989), also prove that Os solubility in laurite increases with decreasing temperature and/or increasing fS_2.

Because fS_2 tends to increase upon cooling, normal patterns of zoning in laurite–erlichmanite grains would record different steps of the crystallization history of these PGM before their entrapment by chromite (Melcher *et al.*, 1997; Garuti *et al.*, 1999a). Nevertheless a continuous decrease in temperature and increase in fS_2 can neither explain the reverse nor the oscillatory patterns of zoning shown by some laurite–erlichmanite grains (Fig. 2, 3 and 4). To account for such chemical variations (including increases in the arsenic concentration to form irarsite), it is necessary to invoke a mechanism capable of creating different fS_2 gradients in space and/or time, with or without changes in temperature, and in a short time before the PGM were trapped by chromite. Variable fS_2 gradients could be generated during the crystallization of chromite by magma mixing (Irvine, 1975, 1977; Arai & Yurimoto, 1994; Zhou *et al.*, 1996; Ballhaus, 1998; Gervilla *et al.*, 2005) or as a consequence of the segregation of a fluid phase from the parent silicate melt (Matveev & Ballhaus, 2002).

Ballhaus (1998) has suggested that chromite crystallization takes place in a hybrid magma formed during mingling (before complete mixing) of two melts with different silica activities in turbulent magma conduits to shallow lithosphere levels (Fig. 6-1a). Any batch of new melt injected in the conduit will mingle turbulently with the pooled melt because of the viscosity contrast of the two melts. This will create chemical differences in each melt bubble crystallizing variable proportions of chromite (Fig. 6-1b). In contrast Matveev & Ballhaus (2002) show that the formation of ophiolite chromitites involves equilibration between an olivine-chromite saturated basaltic melt and an aqueous phase. Decompressing of a water-saturated basalt melt induces the exsolution of a fluid phase (Shaw, 1972; Bottinga & Weill, 1972; Ballhaus, 1998). Given the affinity of a water-rich fluid to oxide surfaces, the segregated fluid tend to use chromite microphenocrystals dispersed in the

Table 3. Representative analyses of zoned laurites and associated minerals from the investigated chromitites.

No. analysis	Mineral	Os	Ir	Ru	Pt	Pd	Rh	Fe	Cr	Ni	S	As	Total
Raw analyses (wt%)													
1	*Laurite*	10.81	4.76	47.19	0.00	0.00	0.30	0.56	1.66	0.11	33.74	0.00	99.13
2	*Os-Laurite*	33.44	4.49	29.97	0.00	0.00	0.29	0.70	1.91	0.05	31.06	0.00	101.91
3	*Laurite*	10.15	4.60	46.09	0.00	0.00	1.65	0.64	2.01	0.10	32.91	1.63	99.78
4	*Irarsite*	2.17	46.18	9.52	0.00	0.00	4.15	0.80	2.52	0.09	15.14	19.94	100.51
5	*Os-Laurite*	23.96	3.41	33.16	0.00	0.00	0.20	1.84	4.26	0.03	29.81	0.00	96.67
6	*Os-Laurite*	25.67	3.21	35.39	0.00	0.00	0.33	0.94	1.99	0.05	32.18	0.00	99.76
7	*Os-Laurite*	25.46	3.13	35.73	0.07	0.00	0.27	1.03	2.02	0.07	32.05	0.00	99.83
8	*Laurite*	7.54	2.20	49.29	0.03	0.00	0.19	0.63	5.80	0.02	34.09	0.00	99.79
9	*Laurite*	9.47	3.51	46.97	0.00	0.00	0.27	0.34	3.00	0.07	34.30	0.00	97.93
10	*Os-Laurite*	21.50	5.07	39.15	0.00	0.00	0.24	0.92	1.63	0.06	32.90	0.00	101.47
11	*Os-Laurite*	21.55	4.64	38.70	0.00	0.00	0.25	0.86	1.40	0.10	32.82	0.00	100.32
12	*Os-Laurite*	22.05	4.76	38.63	0.00	0.00	0.26	0.85	1.29	0.07	33.19	0.00	101.10
13	*Laurite*	7.27	2.19	52.43	0.04	0.00	0.33	0.53	1.17	0.07	35.88	0.00	99.91
14	*Laurite*	6.20	1.75	54.75	0.00	0.00	0.32	0.51	1.23	0.01	35.62	0.00	100.39
15	*Laurite*	5.20	1.73	55.46	0.01	0.00	0.35	0.72	1.44	0.23	34.89	1.68	101.71
16	*Laurite*	18.48	4.17	46.53	0.00	0.00	0.21	0.78	1.63	0.07	36.12	0.00	107.99
17	*Osmium*	78.58	15.85	2.91	0.00	0.00	0.09	1.42	2.40	0.09	0.02	0.00	101.36
18	*Osmium*	77.58	15.49	2.46	0.00	0.00	0.08	1.29	2.33	0.11	0.00	0.00	99.34
19	*Osmium*	76.60	16.05	6.29	0.02	0.00	0.11	1.29	2.32	0.06	0.02	0.00	102.76
20	*Os-Laurite*	21.14	5.05	37.99	0.00	0.03	0.28	0.34	0.44	0.26	33.47	0.00	99.00
21	*Os-Laurite*	23.47	5.19	36.42	0.13	0.08	0.31	0.10	0.45	0.15	33.04	0.00	99.32
22	*Os-Laurite*	21.63	5.17	36.94	0.16	0.00	0.16	0.19	0.39	0.18	32.94	0.02	97.77
23	*Os-Laurite*	22.87	5.12	36.22	0.14	0.00	0.41	0.45	0.42	0.11	33.15	0.03	98.90
24	*Os-Laurite*	23.71	5.36	35.70	0.15	0.00	0.22	0.12	0.44	0.16	33.08	0.00	98.94
25	*Os-Laurite*	23.99	6.15	34.87	0.33	0.00	0.42	0.37	0.50	0.12	33.62	0.03	100.39
26	*Laurite*	18.11	7.63	38.26	0.23	0.21	0.40	0.07	0.57	0.16	33.85	0.09	99.56
27	*Laurite*	18.12	7.16	37.48	0.00	0.22	0.26	0.40	0.64	0.12	33.73	0.00	98.11
28	*Laurite*	18.34	7.36	38.00	0.27	0.00	0.39	0.20	0.13	0.16	33.38	0.00	98.23
29	*Laurite*	18.47	7.34	37.47	0.15	0.00	0.48	0.07	0.66	0.12	33.74	0.00	98.49
30	*Laurite*	19.38	7.18	37.41	0.12	0.00	0.46	0.39	0.79	0.19	33.28	0.02	99.19
Recalculated analyses (wt%)													
1	Laurite	11.15	4.91	48.69	0.00	0.00	0.31	0.01		0.11	34.81	0.00	
2	*Os-Laurite*	33.65	4.52	30.16	0.00	0.00	0.29	0.07		0.05	31.26	0.00	
3	*Laurite*	10.45	4.74	47.45	0.00	0.00	1.70	0.00		0.10	33.88	1.68	
4	*Irarsite*	2.23	47.52	9.80	0.00	0.00	4.27	0.00		0.09	15.58	20.52	
5	*Os-Laurite*	26.04	3.71	36.03	0.00	0.00	0.22	1.58		0.03	32.39	0.00	
6	*Os-Laurite*	26.30	3.29	36.26	0.00	0.00	0.34	0.78		0.05	32.97	0.00	
7	*Os-Laurite*	26.08	3.21	36.60	0.07	0.00	0.28	0.87		0.07	32.83	0.00	
8	*Laurite*	8.08	2.36	52.80	0.03	0.00	0.20	0.00		0.02	36.51	0.00	
9	*Laurite*	10.01	3.71	49.66	0.00	0.00	0.29	0.00		0.07	36.26	0.00	
10	*Os-Laurite*	21.57	5.09	39.27	0.00	0.00	0.24	0.78		0.06	33.00	0.00	
11	*Os-Laurite*	21.81	4.70	39.17	0.00	0.00	0.25	0.74		0.10	33.22	0.00	
12	*Os-Laurite*	22.12	4.77	38.75	0.00	0.00	0.26	0.74		0.07	33.29	0.00	
13	*Laurite*	7.37	2.22	53.16	0.04	0.00	0.33	0.43		0.07	36.38	0.00	
14	*Laurite*	6.26	1.77	55.28	0.00	0.00	0.32	0.40		0.01	35.96	0.00	
15	*Laurite*	5.19	1.73	55.38	0.01	0.00	0.35	0.59		0.23	34.84	1.68	
16	*Laurite*	17.40	3.93	43.81	0.00	0.00	0.20	0.60		0.07	34.01	0.00	
17	*Osmium*	79.58	16.05	2.95	0.00	0.00	0.09	1.22		0.09	0.02	0.00	
18	*Osmium*	80.14	16.00	2.54	0.00	0.00	0.08	1.12		0.11	0.00	0.00	
19	*Osmium*	76.42	16.01	6.28	0.02	0.00	0.11	1.08		0.06	0.02	0.00	
20	*Os-Laurite*	21.52	5.15	38.68	0.00	0.03	0.28	0.00		0.27	34.07	0.00	
21	*Os-Laurite*	23.76	5.25	36.87	0.13	0.08	0.32	0.00		0.15	33.45	0.00	
22	*Os-Laurite*	22.26	5.32	38.01	0.17	0.00	0.16	0.00		0.18	33.89	0.02	
23	*Os-Laurite*	23.33	5.22	36.94	0.14	0.00	0.41	0.00		0.11	33.81	0.03	
24	*Os-Laurite*	24.10	5.45	36.29	0.16	0.00	0.22	0.00		0.16	33.62	0.00	
25	*Os-Laurite*	24.10	6.17	35.04	0.33	0.00	0.43	0.00		0.12	33.78	0.03	
26	*Laurite*	18.31	7.71	38.67	0.23	0.21	0.41	0.00		0.16	34.22	0.09	
27	*Laurite*	18.67	7.37	38.61	0.00	0.22	0.26	0.00		0.12	34.75	0.00	
28	*Laurite*	18.73	7.52	38.82	0.27	0.00	0.39	0.00		0.16	34.10	0.00	
29	*Laurite*	18.90	7.51	38.32	0.15	0.00	0.49	0.00		0.12	34.51	0.00	
30	*Laurite*	19.77	7.32	38.16	0.12	0.00	0.47	0.00		0.19	33.95	0.02	

Table 3. Continued

No. analysis	Mineral	Os	Ir	Ru	Pt	Pd	Rh	Fe	Cr	Ni	S	As	Total
Atomis percentages													
1	Laurite	3.54	1.54	29.08	0.00	0.00	0.18	0.01		0.12	65.53	0.00	
2	*Os-Laurite*	11.97	1.59	20.18	0.00	0.00	0.19	0.08		0.06	65.93	0.00	
3	*Laurite*	3.34	1.50	28.52	0.00	0.00	1.00	0.00		0.11	64.18	1.36	
4	*Irarsite*	1.01	21.34	8.37	0.00	0.00	3.58	0.00		0.14	41.93	23.64	
5	*Os-Laurite*	8.81	1.24	22.95	0.00	0.00	0.14	1.82		0.04	65.01	0.00	
6	*Os-Laurite*	8.86	1.10	22.99	0.00	0.00	0.21	0.89		0.06	65.89	0.00	
7	*Os-Laurite*	8.79	1.07	23.22	0.02	0.00	0.17	1.00		0.08	65.65	0.00	
8	*Laurite*	2.47	0.71	30.40	0.01	0.00	0.12	0.00		0.02	66.27	0.00	
9	*Laurite*	3.10	1.14	28.93	0.00	0.00	0.16	0.00		0.07	66.59	0.00	
10	*Os-Laurite*	7.20	1.68	24.67	0.00	0.00	0.15	0.88		0.07	65.35	0.00	
11	*Os-Laurite*	7.26	1.55	24.53	0.00	0.00	0.16	0.84		0.11	65.56	0.00	
12	*Os-Laurite*	7.36	1.57	24.27	0.00	0.00	0.16	0.83		0.08	65.72	0.00	
13	*Laurite*	2.25	0.67	30.53	0.01	0.00	0.19	0.45		0.07	65.84	0.00	
14	*Laurite*	1.91	0.53	31.78	0.00	0.00	0.18	0.42		0.01	65.16	0.00	
15	*Laurite*	1.60	0.53	32.03	0.00	0.00	0.20	0.62		0.23	63.50	1.31	
16	*Laurite*	5.65	1.26	26.76	0.00	0.00	0.12	0.66		0.07	65.48	0.00	
17	*Osmium*	75.25	15.02	5.25	0.00	0.00	0.16	3.93		0.28	0.11	0.00	
18	*Osmium*	76.27	15.07	4.55	0.00	0.00	0.15	3.62		0.35	0.00	0.00	
19	*Osmium*	70.57	14.63	10.91	0.02	0.00	0.19	3.39		0.18	0.11	0.00	
20	*Os-Laurite*	7.10	1.68	24.03	0.00	0.02	0.17	0.00		0.29	66.71	0.00	
21	*Os-Laurite*	7.97	1.74	23.28	0.04	0.05	0.20	0.00		0.16	66.56	0.00	
22	*Os-Laurite*	7.39	1.75	23.75	0.05	0.00	0.10	0.00		0.19	66.75	0.01	
23	*Os-Laurite*	7.78	1.72	23.18	0.05	0.00	0.25	0.00		0.12	66.87	0.03	
24	*Os-Laurite*	8.08	1.81	22.89	0.05	0.00	0.14	0.00		0.18	66.85	0.00	
25	*Os-Laurite*	8.08	2.05	22.12	0.11	0.00	0.26	0.00		0.13	67.22	0.02	
26	*Laurite*	6.03	2.51	23.96	0.07	0.12	0.25	0.00		0.17	66.81	0.08	
27	*Laurite*	6.10	2.38	23.75	0.00	0.13	0.16	0.00		0.13	67.35	0.00	
28	*Laurite*	6.18	2.46	24.11	0.09	0.00	0.24	0.00		0.17	66.75	0.00	
29	*Laurite*	6.20	2.44	23.68	0.05	0.00	0.30	0.00		0.13	67.20	0.00	
30	*Laurite*	6.55	2.40	23.79	0.04	0.00	0.29	0.00		0.20	66.71	0.02	

Monte Bueno Mine: 1–4. Dobromirtsi: 5–19. Caridad Mine: 20–30.

melt as nucleation sites (Matveev & Ballhaus, 2002) scavenging chromite from the melt (Fig. 6-2a).

In any of the two models, coalescence of chromite-rich melt/fluid bubbles promoted by the existence of a turbulent regime should lead to joint chromite forming larger crystals (Fig. 6-1b, 6-2b). Such a regime can be caused by periodic inputs of melt batches within a conduit, similar to that proposed by Lago *et al*. (1982). The denser chromite-bearing bubbles will be transported to the walls of the conduits (Matveev & Ballhaus, 2002), like in the elutriation cell described by Lago *et al*. (1982), promoting their coalescence and partial solidification (note that the solid wall-rock can be ~200 °C cooler than the melt). In both models, each melt/fluid bubble will retain its own chemical composition, fO_2 and fS_2 until it coalesces with another bubble. This may create the heterogeneous, variable environment necessary to form the different patterns of zoning in laurite–erlichmanite grains.

Because Cr^{3+} and Fe^{3+} partition preferentially into chromite, each chromite nucleus may create a reduced boundary layer enveloping the nucleus and cause saturation of the most oxidized PGE species (Os, Ru and very probably Ir) in the melt/fluid (Mungall, 2002, 2005; Ballhaus *et al.*, 2006; Finnigan *et al.*, 2008). Due to their pronounced affinity to the chromite surface, these PGE will crystallize on chromite surfaces, being fractionated along with chromite (Ballhaus *et al.*, 2006). Such physical fractionation may take place in the form of extremely small-sized metallic nuggets of Os, Ru and Ir (Ballhaus *et al*., 2006) and/or submicroscopic grains (or clusters) of Os-Ru alloys which would also incorporate Ir (Tredoux *et al.*, 1995; Gervilla *et al.*, 2005) (Fig. 6-3). In this scenario, the Os-, Ru-, Ir-metallic nuggets and submicroscopic Os-Ru-Ir alloys keep attached to chromite grain boundaries (Bockrath *et al.*, 2004; Mungall, 2005; Ballhaus *et al*., 2006) in equilibrium with the closest surrounding melt/fluid. Weak increases in fO_2 and fS_2, as a consequence of coalescence of Os-, Ir-, and Ru- and chromite-bearing melt/fluid bubbles, can promote crystallization of laurite directly from the melt/fluid or, more probably, by reaction with the already formed Os-Ir-Ru alloys (Bockrath *et al*., 2004) (Fig. 6-3). Crystallization of laurite by alloy-melt reactions may also occur during hiatuses in chromite growth. Later PGM will be incorporated into chromite grains if they begin to grow again during fluctuations of the turbulent regime (Kinnaird *et al*., 2002). The composition of laurite, as well as the local presence of irarsite, will mainly depend on fS_2 conditions and As

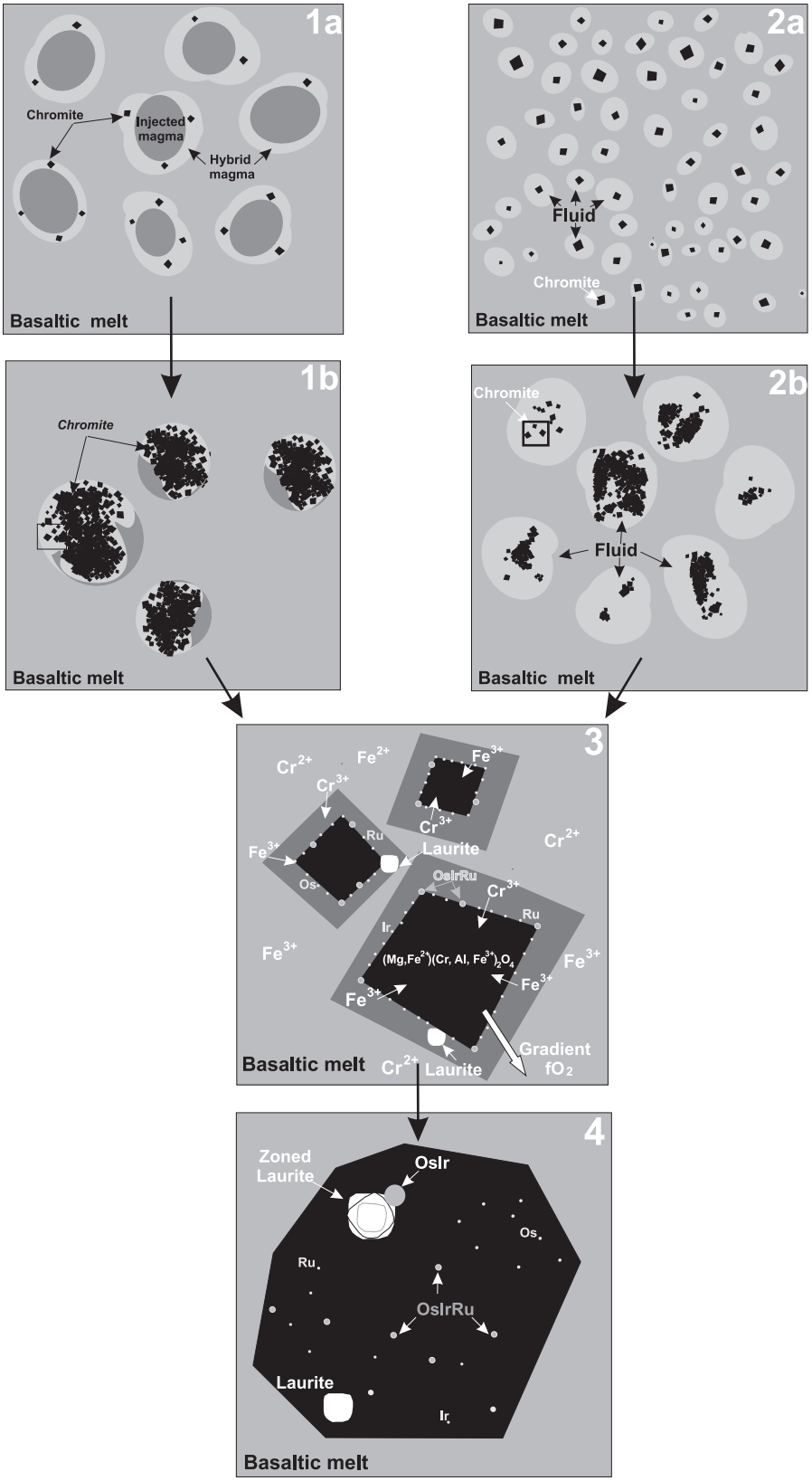

Fig. 6. Sketches showing different steps of chromite crystallization and platinum-group element fractionation to form platinum-group minerals (PGM), from a basaltic melt. (1a) Crystallization of chromite from a hybrid magma. (1b) Chromite accumulation in each individual bubble. (2a) Nucleation of exsolving fluid phase on dispersed chromite microphenocrystals. (2b) Coalescence of chromite-laden fluid bubbles and chromite accumulation. (3) Precipitation of Os, Ru and Ir as extremely small-sized metallic nuggets and/or OsIrRu alloys from the melt as a consequence of changing redox conditions in the periphery of growing chromite crystal. Note that laurite crystals also form close to chromite boundaries. (4) Physical trapping of PGM by chromite.

concentration. The latter will change during bubble coalescence. Progressive bubble coalescence and chromite growth give rise to the formation of larger chromite crystals, trapping the PGM attached to the edges of chromite nuclei and preventing any further chemical exchange between PGM and the surrounding melt/fluid (Fig. 6-4).

According to the above proposed model, Os-Ir-Ru alloys, laurite–erlichmanite with different Ru/(Ru + Os) ratios, and occasionally irarsite, may coexist at the same time but in different zones of the chromite body (they frequently coexist in a single sample) (Fig. 6-4). Note that Os-Ir alloys only occur attached to Os-poor laurite rims in reverse zoned grains, recording the equilibrium temperature and fS_2 conditions determined experimentally by Brenan & Andrews (2001).

The inclusions of Ni-Cu-Fe sulphides in the zoned laurite–erlichmanite grain studied from Caridad (Fig. 4), and in many other, non-zoned grains from the same deposit can be interpreted as droplets of an immiscible sulphide melt segregated from the hybrid silicate melt, and trapped by the growing laurite–erlichmanite. This shows that fS_2 can suddenly increase during the crystallization of laurite–erlichmanite up to the level of sulphur saturation. This again supports crystallization of laurite in an open environment liable to rapid and sudden chemical and thermodynamic changes.

The origin of oscillatory zoned grains of laurite–erlichmanite enveloped by zoned irarsite–hollingworthite and vysotskite–braggite from the Penikat layered complex (Finland) has been ascribed to rapid fluctuations in fS_2 during their sequential crystallization from a melt in a closed system (Barkov *et al*., 2004). However, while all the grains studied by these authors show growth-related zones parallel to crystal faces and always exhibit the same crystallization order, many of the grains reported here show rounded shapes and different crystallization sequences. In addition, in some PGM assemblages laurite overgrowths on late irarsite crystals and some laurite grains contain inclusions of droplets of an immiscible Ni-Cu-Fe sulphide melt. Barkov *et al*. (2004) did not explain the origin of the assumed fluctuation in fS_2 in a closed system. Similarly, Moreno *et al*. (1999) and Grieco *et al*. (2006) interpret some zoning patterns as the result of subsolidus cooling or post-crystallization rearranging of Os and Ru in the sealed inclusions. However, the growth features (some of them forming part of complex oscillatory patterns) in the zoned grains reported here suggest that the formation of these patterns took place in an open rather than a closed system. As a consequence, we consider that zoning patterns in laurite–erlichmanite (with or without irarsite) inclusions in fresh chromite from ophiolite chromitites form in an open magmatic environment. This environment is characterized by growth processes, related to a heterogeneous, variable chemical environment, created by the turbulent regime generated by the intrusion of different batches of melt.

The fact that irarsite only grows at corners and edges of laurite–erlichmanite grains indicates that the supersaturation of its components in the melt was too low for the formation of its own nuclei. In this situation the laurite–erlichmanite surface and especially the corners and edges (with their highest attachment force) acts as nucleation seeds. However, even with the help of the laurite–erlichmanite seed, irarsite components supersaturation keeps low and reaches values required for the nucleation only twice, after some abrupt events (marked by respective zone boundaries in laurite–erlichmanite). On Fig. 2a, right below the irarsite, there is a complete cub-octahedral epitactic laurite individual. On Fig. 2b, the growth of irarsite causes splitting of laurite–erlichmanite into three parallel subindividuals, forming the so called inductive boundary. This kinked boundary is typical for contemporary, concurrent growth of two species with comparable growth power.

6.2. Preservation of zoning

Laurite and erlichmanite have the same cubic *Pa*3, pyrite-type structure and a complete solid-solution series exists between the two end-members (Leonard *et al.*, 1969; Snetsinger, 1971; Harris, 1974; Begizov *et al.*, 1976; Bowles *et al.*, 1983; Cabri, 2002). As laurite–erlichmanite forms at a very high temperature (~1250 °C; Brenan & Andrews, 2001), chemically homogeneous grains, equilibrated by intracrystalline diffusion of Os and Ru on cooling would be expected. Unfortunately, there are no experimental data on diffusion coefficients of Os and Ru in a pyrite-type structure. However, it is known that pyrite-type structures have very strong covalent bonds, characterized by very high detachment energies (Vaughan & Craig, 1978). Considerable energy must be added to the system in order to move the metal from one position to another. Thus, intracrystalline diffusion would take place only on heating, not on cooling, especially if the rate of cooling was relatively fast (quenching effect).

In this scenario, we consider that each growth zone of a laurite–erlichmanite crystal has a preserved composition in equilibrium with the environment at the time of its formation. If there is no change in the environment during the whole growth period, the crystal becomes compositionally uniform. This is more probable for short growth periods and could be the case for most laurite–erlichmanite crystals reported in ophiolite chromitites. In contrast, if growth lasts longer, some abrupt event will happen sooner or later in the environment and zoning will appear. Composition will change without any zonal boundary or through a very fine scale zoning if the environment changes very steadily, without abrupt events. Thus, the patterns of zoning of laurite–erlichmanite described in this paper can be interpreted as a consequence of primary magmatic zoning, generated in a turbulent environment of crystallization (with changes in fS_2, fO_2 and temperature) preserved in specific areas of the chromitite body. These areas probably cooled faster than the rest of the body. This might occur near the cooler peridotitic walls of the chamber (or in small-sized chambers, like those of Monte Bueno) where heat diffusion would create steep temperature gradients favouring the relatively fast cooling of PGM and chromite.

7. Concluding remarks

(1) On the basis of chemical zoning sequences, three different patterns of zoning have been distinguished: (i) grains with Os-poor laurite cores and Os-rich laurite rims (normal zoning), (ii) grains with Os-rich laurite cores and Os-poor laurite rims (reverse zoning) and (iii) grains made up of alternating Os-rich, Os-poor laurite and erlichmanite (oscillatory zoning).

(2) Zoning is interpreted mainly as the result of changes in fS_2, fO_2 and temperature of the melt before PGM trapping in chromite.

(3) The environment capable of producing sharp changes in physicochemical conditions can be obtained during crystallization of chromite by magma mingling with or without segregation of a fluid-rich fraction.

(4) Preservation of the zoning patterns is interpreted here as a consequence of low diffusion rates of Ru and Os in pyrite-type structures and relatively fast cooling rates.

Acknowledgments: The authors are grateful to K.S. Periov local chief geologist for his help and attention during field works in the Dobromirtsi area, and to R. Ruiz Sánchez and J. Blanco Moreno during field work in the Sagua de Tánamo region. We wish to acknowledge the assistance of A. Rueda Torres (Department of Mineralogy and Petrology, University of Granada) for the preparation of the polished sections and the assistance of X. Llovet (Serveis Científico-Tècnics of the University of Barcelona), C. Gilles (Analysis and Mineral Characterization Laboratory of BRGM, Orléans, France), I. Sánchez Almazo (Centro Andaluz de Medio Ambiente of the Junta Andalucía-University of Granada), A. González Segura (Centro de Instrumentación Científica of the University of Granada) for their assistance with EPMA, ESEM and FESEM, respectively. Likewise we acknowledge Daniel Cooper for his help with the English language. This research has been financially supported by the Spanish project CGL2007-61205 of the MEC and PROMES-RESRO1 of the BRGM, France, the research group (RNM 131) of the Junta de Andalucía, and F.P.I grant BES-2005-8328 of the Spanish Ministry of Education and Sciences.

References

Ahmed, A.H. & Arai, S. (2003a): Platinum-group element mineralogy of late Proterozoic podiform chromitites from the Eastern Desert of Egypt: a preliminary result. *in* ''Mineral exploration and sustainable development'', Eliopoulos *et al*., ed. Milpress, Rotterdam.

—, — (2003b): Platinum-group minerals in podiforms chromitites of the Oman ophiolite. *Can. Mineral.*, **41**, 597–616.

Amossé, J., Allibert, M., Fisher, W., Piboule, M. (1990): Experimental study of the solubility of platinum and iridium in basic silicate melts – implications for the differentiation of platinum-group elements during magmatic processes. *Chem. Geol*., **81**, 45–53.

Amossé, J., Dable, P., Allibert, M. (2000): Thermochemical behavior of Pt, Ir, Rh and Ru *vs.* fO2 and fS2 in a basaltic melt. Implications for the differentiation and precipitation of these elements. *Mineral. Petrol*., **68**, 9–62.

Andrews, D.R.A. & Brenan, J.M. (2002): Phase-equilibrium constraints on the magmatic origin of laurite + Ru-Os-Ir alloy. *Can. Mineral*., **40**, 1705–1716.

Arai, S. & Yurimoto, H. (1994): Podiform chromitites of the Tari-Misaka ultramafic complex, southwest Japan, as mantle-melt interaction products. *Econ. Geol*., **89**, 1279–1288.

Augé, T. (1985): Platinum-group mineral inclusions in ophiolitic chromitite from the Vourinos Complex. Greece. *Can. Mineral*., **23**, 163–171.

— (1988): Platinum-group minerals in the Tiébaghi and Vourinos ophiolite complexes: genetic implications. *Can. Mineral*., **26**, 177–192.

Augé, T. & Johan, Z. (1988): Comparative study of chromite deposits from Troodos, Vourinos, North Oman and New Caledonia ophiolites. *in* ''Mineral deposits in the European community'', J. Boissonnas & P. Omenetto, Eds. Springer-Verlag, Heidelberg, 267–288.

Ballhaus, C. (1998). Origin of podiform chromite deposits by magma mingling. *Earth Planet. Sci. Lett.*, **156**, 185–193.

Ballhaus, C. & Sylvester, P. (2000): Noble metal enrichment processes in the Merensky Reef, Bushveld Complex. *J. Petrol*., **41**, 545–561.

Ballhaus, C., Bockrath, C., Wohlegemuth-Uberwasser, C., Laurenz, V., Berndt J. (2006): Fractionation of the noble metals by physical processes. *Contrib. Mineral. Petrol*., **152**, 667–684.

Barin, I. (1989): Thermochemical data of pure substances. Publisher: VCH, Weinheim, Fed. Rep. Ger., 1829 p.

Barkov, A., Fleet, M.E., Martin, R.F., Alapieti, T.T. (2004): Zoned sulphides and sulpharsenides of the platinum-group elements from the Penikat layered complex, Finland. *Can. Mineral*., **42**, 515–537.

Begizov, V.D., Zaýyalov, E.N., Khostova, V.P. (1976): Minerals of the erlichmanite-laurite and hollingworthite-irarsite series from Ural placers. *Zap. Vses. Mineral. Obshch*., **105**, 213–218.

Brenan, J.M. & Andrews, D. (2001): High-temperature stability of laurite and Ru-Os-Ir alloy and their role in PGE fractionation in mafic magmas. *Can. Mineral*., **39**, 341–360.

Bockrath, C., Ballhaus, C., Holzheid, A. (2004): Stabilities of laurite RuS_2 and monosulphide liquid solution at magmatic temperature. *Chem. Geol*., **208**, 265–271.

Bottinga, Y. & Weill, D.F. (1972): The viscosity of magmatic silicate liquids: a model for calculation. *Am. J. Sci.*, **272**, 438–475.

Bowles, J.F.W., Atkin, D., Lambert, J.L.M., Deans, T., Philips, R. (1983): The chemistry, reflectance, and cell size of the erlichmanite (OsS_2)- laurite (RuS_2) series. *Mineral. Mag*., **47**, 465–471.

Cabri, L.J. (2002): The geology, geochemistry, mineralogy and mineral beneficiation of platinum-group minerals. Can. Inst. Min. Metall. Petrol. Calgary, Alberta, Canada, 852 p.

Capobianco, C.J. & Drake, M.J. (1990): Partitioning of ruthenium, rhodium and palladium between spinel and silicate melt and implications for platinum-group elements fractionation trends. *Geochim. Cosmochim. Acta*., **54**, 869–874.

Capobianco, C.J., Herving, R.L., Drake, M.J. (1994): Experiments on crystal liquid partitioning of Ru, rh, and Pd from magnetite and hematite solid-solutions crystallized from silicate melt. *Chem. Geol*., **113**, 23–43.

Corrivaux, L. & Laflamme, J.H.G. (1990): Minéralogie des éléments du groupe du platine dans les chromitites de Íophiolite de Therford Mines, Québec. *Can. Mineral*., **28**, 579–595.

Finnigan, C.S., Brenan, J.M., Mungall, J.E. & McDonough, W.F. (2008): Experiments and models bearing on the role of chromite as a collector of platinum group minerals by local reduction. *J. Petrol*., doi:10.1093/petrology/egn041.

Garuti, G., Zaccarini, F., Moloshag, V., Alimov, V. (1999a): Platinum-group elements as indicators of sulphur fugacity in ophiolitic upper mantle: an example from chromitites of the Ray-Iz ultramafic complex, Polar Urals, Russia. *Can. Mineral*., **37**, 1099–1115.

Garuti, G., Zaccarini, F., Economou-Eliopoulos, M. (1999b): Paragenesis and composition of laurite from chromitites of Othrys (Greece): implications for Os-Ru fractionation in ophiolitic upper mantle of the Balkan peninsula. *Mineral. Dep*., **34**, 312–319.

Gauthier, M., Corrivaux, L., Trottier, L.J., Cabri, J., Laflamme, J.H.G., Bergeron, M. (1990): Chromitites platinifères des complexes ophiolitiques de ÍEstrie-Beauce, Appalaches du Sud du Québec. *Mineral. Dep*., **25**, 169–178.

Gervilla, F., Proenza, J.A., Frei, R., González-Jiménez, J.M., Garrido, C.J., Melgarejo, J.C., Meibom, A., Díaz-Martínez, R., Lavaut, W. (2005): Distribution of platinum-group elements and Os isotopes in chromite ores from Mayarí-Baracoa Ophiolitic Belt (eastern Cuba). *Contrib. Mineral. Petrol*., **150**, 589–607.

Grieco, G., Diella, V., Chaplygina, N.L., Savalieva, G.N. (2006): Platinum group elements zoning and mineralogy of chromitite from the cumulate sequence of the Nurali massif (Southern Urals, Russia). *Ore. Geol. Rev*., **30**, 1–3, 257–276.

González-Jiménez, J.M., Gervilla, F., Kerestedjian, T., Proenza, J.A. (2007): Postmagmatic evolution of platinum-group and base-metal mineral assemblages in Paleozoic ophiolitic chromitites from the Dobromirtsi massif, Rhodope Mountains (SE Bulgaria). *in* ''Mineral exploration and research: digging deeper'', C.J. Andrew, *et al*., ed. Irish Association of Economic Geology, Ireland, 889–892.

Gutierrez-Narbona, R., Lorand, J.-P., Gervilla, F, Gros, M. (2003): New data on base metal mineralogy and platinum-group minerals in the Ojen chromitites (Serrania de Ronda, Betic Cordillera, southern Spain). *N. Jb. Miner. Abh*., **179**, 143–173.

Harris, D.C. (1974): Ruthenarsenite and iridarsenite, two new minerals from the territory of Papua and New Guinea and associated irarsite and cubic iron-bearing platinum. *Can. Mineral*., **12**, 280–284.

Irvine, T.N. (1975): Chromite crystallization in the joint Mg_2SiO_4-$CaMgSi_2O_8$-$MgCr_2O_4$-SiO_2. *Carnegie Instit. Washington Yearbook*, **76**, 465–472.

— (1977): Origin of chromitite in the Muskov intrusion and other stratiform intrusions: a new interpretation. *Geol*., **5**, 273–277.

Iturralde-Vinent, M.A., Díaz-Otero, C., Rodríguez-Vega, A., Díaz-Martínez, R. (2006): Tectonic implications of paleontologic dating of Cretaceous-Danian sections of Eastern Cuba. *Geol. Act.*, 4, 1–2, 89–102.

Kerestedjian, T., Gervilla, F., González-Jiménez, J.M., Proenza, J.A. (2006): New data on chromitites from Dobromirtsi, Eastern Rhodopes. *in* ''Proceedings of National conference Geosciences 2006'', Sofia 30.11.-01.12.2006, 255–258.

Kinnaird, A., Kruger, F.J., Nex, P.A.M., Cawthorn, R.G. (2002): Chromite formation – a key to understanding processes of platinum enrichment. *Trans. Inst. Min. Metal.*, **11**, B23–B35.

Lago, B., Rabinowicz, M., Nicolas, A. (1982): Podiform chromite ore bodies: a genetic model. *J. Petrol*., **23**, 103–125.

Legendre, O. & Augé, T. (1986): Mineralogy of platinum group minerals inclusions in chromitites from different ophiolitic complexes. *in* ''Metallogeny of basic and ultrabasic rocks'', M.J. Gallagher, R.A. Ixer, C.R. Neary, H.M. Prichard, eds. Institution of Mining and Metallurgy, London, U.K., 361–372.

Leonard, B.F., Desborough, G.A., Page, N.J. (1969): Ore microscopy and chemical composition of some laurites. *Am. Mineral*., **54**, 1330–1340.

Marchesi, C., Garrido, C.J., Godard, M., Proenza, J.A., Gervilla, F., Blanco-Moreno, J. (2006): Petrogenesis of highly depleted peridotites and gabbroic rocks from the Mayarí-Baracoa Ophiolitic Belt (eastern Cuba). *Contrib. Mineral. Petrol*., **151**, 717–736.

Matveev, S. & Ballhaus, C. (2002): Role of water in the origin of podiform chromitite deposits. *Earth. Planet. Sc. Lett*., **203**, 235–243.

Melcher, F., Grum, W., Simon, G., Thalhammer, T.V., E.F. Stumpfl, (1997): Petrogenesis of the ophiolitic giant chromite deposits of Kempirsai, Kazakhstan: a study of solid and fluid inclusions in chromite. *J. Petrol*., **38**, 1419–1458.

Moreno, T., Prichard, H.M., Lunar, R., Monterrubio, S., Fisher, P. (1999): Formation of a secondary PGM assemblage chromitites from the Herbeira ultramafic massif in Cabo Ortegal, NW Spain. *Eur. J. Mineral*., **11**, 363–378.

Murashko, V.I. & Lavandero, R.M. (1989): Chromite in the hyperbasite belt of Cuba. *Int. Geol. Rev.*, **31**, 90–99.

Mungall, J.E. (2002): A model for coprecipitation of platinum-group minerals with chromite from silicate melts. *in* ''9th international platinum symposium'', abstract with program, 21–25 July 2002, Billings, Montana, 321–324.

— (2005): Magmatic geochemistry of the Platinum-group elements. *in* ''Exploration from Platinum-group elements deposits''. Short Course Series – Mineralogical Association of Canada, **35**, 1–34.

Nakagawa, M. & Franco, H.E.A. (1997): Placer Ru-Os-Ir alloys and sulphides: indicators of sulphur fugacity in an ophiolite? *Can. Mineral*., **35**, 1441–1452.

Ovtcharova, M., von Quadt, A., Heinrich, C., Frank, M., Rohrmeier, M., Peytcheva, I., Neubauer, F. (2001): Late alpine extensional stage of the central Rhodopian core complex and related acid magmatism (Madan Dome, Bulgaria): isotope and geochronological data. *in* ''Mineral deposits at the beginning of the 21st century'', Piestrynski, *et al*. eds. Balkema, Rotterdam, 551–553.

Proenza, J.A., Gervilla, F., Melgarejo, J.C., Bodinier, J.L. (1999): Al- and Cr- rich chromitites from the Mayarí-Baracoa Ophiolite Belt (eastern Cuba): consequence of interaction between volatile-rich melts and peridotite in suprasubduction mantle. *Econ. Geol*., **94**, 547–566.

Proenza, J.A., Melgarejo, J.C., Gervilla, F., Rodriguez-Vega, A., Díaz Martínez, R., Ruiz-Sánchez, R., Lavaut, W. (2003): Coexistence of Cr- and Al-rich ophiolitic chromitites in a small area: the Sagua de Tánamo district, Eastern Cuba. *in* ''Mineral exploration and sustainable development''. Eliopoulos D.G. *et al*., eds. Millpress, Rotterdam, Netherlands, 631–634.

Proenza, J.A., Díaz-Martínez, R., Iriondo, A., Marchesi, C., Melgarejo, J.C., Gervilla, F., Garrido, C.J., Rodríguez-Vega,

A., Lozano-Santacruz, R., Blanco-Moreno, J.A. (2006): Primitive island-arc Cretaceous volcanic rocks in eastern Cuba: the Téneme formation. *Geol. Acta*, **4**(1–2), 103–121.

Righter, K., Campbell, A.J., Humayun, M., Herving, R.L. (2004): Partitioning of Ru, Rh, Pd, Re, Ir and Au between Cr-bearing spinel, olivine, pyroxene and silicate melts. *Geochim. Cosmochim. Acta*., **68**, 867–880.

Sattari, P., Brenan, J.M., Horn, I., McDonough, W.F. (2002): Experimental constraints on the sulphide-silicate and chromite-silicate melt partitioning behaviour of rhenium and platinum-group elements. *Econ. Geol*., **97**, 385–398.

Snetsinger, K.G. (1971): Erlichmanite (OsS_2), a new mineral. *Am. Mineral*., **56**, 1501–1506.

Shaw, H.R. (1972): Viscosities of magmatic silicate liquids: an empirical method of prediction. *Am. J. Sci.*, **272**, 870–893.

Stockman, H.W. & Hlava, P. (1984): Platinum-group minerals in alpine chromitites from Southwestern Oregon. *Econ. Geol*., **79**, 491–508.

Tarkian, M., Naidenova, E., Zhelyaskova-Panayotova M. (1991): Platinum-group minerals in chromitites from the Eastern Rhodope Ultramafic complex, Bulgaria. *Mineral. Petrol*., **44**, 73–87.

Tredoux, M., Lindsay, N.M., Davies, G., Macdonald, L. (1995): The fractionation of platinum-group elements in magmatic system, with the suggestion a novel causal mechanism. *South. Africa. J. Geol*., **98**, 157–167.

Torres-Ruiz, J., Garuti, G., Gazzoti, M., Gervilla, F., Fenoll Hach-Alí, P. (1996): Platinum-group minerals in chromitites from the Ojen lherzolite massif (Serranía de Ronda, Betic Cordillera, Southern Spain). *Mineral. Petrol*., **56**, 25–50.

Vaughan, D.J. & Craig, J.R. (1978). Mineral chemistry of metal Sulfides. Cambridge Earth Science Series, Cambridge University Press, Cambridge. 493 p.

Wood, S.A. (1987): Thermodynamic calculations of the volatility of the platinum group elements (PGE): The PGE content of fluids at magmatic temperatures. *Geochim. Cosmochim. Acta*., **51**, 41–3050.

Zaccarini, F., Pushkarev, E.V., Fershtater, B., Garuti, G. (2004): Composition and mineralogy of PGE-rich chromitites in the Nurali lherzolite-gabbro complex, southern Urals, Russia. *Can. Mineral*., **42**, 545–562.

Zhelyaskova-Panayotova, M., Zinzov, Z., Pashov, G. (2000): Hydrothermal gold mineralization in ultrabasites near Dobromirtsi village, Kurdjali region. *Ann. Sofia Univ*., **93**, 1, 173–186 (in Bulgarian).

Zhou, M.F., Robinson, P.T., Malpas, J., Li, Z. (1996): Podiform chromitites in the Luobusa ophiolite (southern Tibet): implications for melt-rock interaction and chromite segregation in the upper mantle. *J. Petrol*., **37**, 3–21.

Received 18 April 2008
Modified version received 28 November 2008
Accepted 19 January 2009